Supporting information

Contrast variation of micelles composed of Ca^{2+} and block copolymers of two negatively charged polyelectrolytes

Nico Carl,[†,‡] Sylvain Prévost,[†] Ralf Schweins,[†] and Klaus Huber[*,‡]

†*Large Scale Structures Group, DS, Institut Laue-Langevin, 71 Avenue des Martyrs, CS 20 156, 38042 Grenoble, France*

‡*Physikalische Chemie, Universität Paderborn, Warburger Str. 100, 33098 Paderborn, Germany*

E-mail: klaus.huber@upb.de

Contents

1 Scattering length densities

Table S1 shows the molar volumes V_m, scattering length b and scattering length densities ρ for neutrons and X-rays (at 12.46 keV) used for the analysis of the data. The scattering length density of a given compound is given by

$$\rho = \frac{b}{V_m} N_a \tag{S1}$$

with N_A being the Avogadro constant.

Table S1: Molar volumes, neutron and X-ray scattering length and scattering length density of the used compounds. $\rho_{\text{X-rays}}$ was calculated for a X-ray energy of 12.46 keV.

Compound	V_m /cm^3 mol^{-1}	b_{neutrons} /fm	$b_{\text{X-Rays}}$ /fm	ρ_{neutrons} /$1 \cdot 10^{10}$ cm^{-2}/	$\rho_{\text{X-rays}}$ /$1 \cdot 10^{14}$ cm^{-2}
h_3PA^-	29.1[a]	20.327	107.269	4.208	22.21
d_3PA^-	29.1[a]	51.557	107.269	10.674	22.21
NaPSS	108.7	50.881	299.823	2.818	16.61
D_2O	18.141	19.145	28.242	6.355	9.375
H_2O	18.069	−1.675	28.242	−0.558	9.398
Ca^{2+}	17.0 ± 2.8[b]	4.7	51.652	1.665	$1.830 \cdot 10^{-3}$
d_3−$PA_{1190}PSS_{70}$[c]				7.789	
h_3−$PA_{1190}PSS_{70}$[c]				3.506	
d_3−$PA_{360}PSS_{400}$[c]				4.200	

[a] Taken from reference 2. [b] The molar volume of Ca^{2+} was fitted. The shown value is the average value we obtained from analysis of the three different polymers. [c] We assumed that every PA monomer is complexed by 0.5 equivalents of Ca^{2+}.

2 Scattering from block copolymer micelles with Gaussian chains in the corona

The form factor for block copolymer micelles with Gaussian chains in the corona was first derived by Pedersen[3]. It assumes a homogeneous core, with Gaussian chains in the corona. The Gaussian chains are displaced from the surface of the core to avoid penetration into the

core. The form factor is given by

$$\frac{d\Sigma}{d\Omega}(q) = N\left[N_{\mathrm{agg}}^2\beta_{\mathrm{core}}^2 A_{\mathrm{core}}^2(q) + N_{\mathrm{agg}}\beta_{\mathrm{corona}}^2 P_{\mathrm{corona}}(q) + 2N_{\mathrm{agg}}^2\beta_{\mathrm{core}}\beta_{\mathrm{corona}} A_{\mathrm{core}}(q) A_{\mathrm{corona}}(q) + N_{\mathrm{agg}}(N_{\mathrm{agg}}-1)\beta_{\mathrm{corona}}^2 A_{\mathrm{corona}}^2(q)\right] \tag{S2}$$

The form factor is similar to the one given in eq 2 of the main manuscript. It contains four different terms: The scattering from the homogeneous core A_{core}^2, the form factor of the chains in the corona $P_{\mathrm{corona}}(q)$, the cross-term between core and chains in the corona $A_{\mathrm{core}}(q) A_{\mathrm{corona}}(q)$ and the cross-term between chains in the corona $A_{\mathrm{corona}}^2(q)$. Furthermore, the pre-factors of the individual terms are the aggregation number of the micelle N_{agg} and the excess scattering length densities of the block forming the spherical core β_{core} and the corona β_{corona}.

A_{core} is given by the scattering amplitude of a homogeneous sphere with radius R_{core}

$$A_{\mathrm{core}}(q) = 3\frac{\sin(qR_{\mathrm{core}}) - qR_{\mathrm{core}}\cos(qR_{\mathrm{core}})}{(qR_{\mathrm{core}})^3} \tag{S3}$$

$P_{\mathrm{corona}}(q)$ is given by the Debye function, describing the form factor of a Gaussian chain with radius of gyration R_g

$$P_{\mathrm{corona}}(q) = \frac{2\left(\exp\left(-q^2R_g^2\right) - 1 + q^2R_g^2\right)}{\left(q^2R_g^2\right)^2} \tag{S4}$$

$A_{\mathrm{corona}}(q)$ is given by

$$A_{\mathrm{corona}}(q) = \frac{1-\exp\left(-q^2R_g^2\right)}{q^2R_g^2}\frac{\sin\left(q\left(R_{\mathrm{core}} + dR_g\right)\right)}{q\left(R_{\mathrm{core}} + dR_g\right)} \tag{S5}$$

The parameter d describes the displacement of the Gaussian chains from the surface of the core and is usually around 1.

In order to take into account the size distribution of micelles we assumed a log-normal

distribution of the aggregation number N_{agg}

$$p\left(N_{\mathrm{agg}}\right) = \frac{1}{H\sqrt{2\pi}N_{\mathrm{agg}}} \exp\left(\frac{-\log\left(N_{\mathrm{agg}} - M\right)^2}{2H^2}\right) \tag{S6}$$

where H and M define the distribution and are connected to the mean aggregation number $\overline{N_{\mathrm{agg}}}$ and standard deviation $\sigma_{\overline{N_{\mathrm{agg}}}}$ by

$$\overline{N_{\mathrm{agg}}} = \exp\left(M + \frac{H^2}{2}\right) \tag{S7}$$

$$\sigma_{\overline{N_{\mathrm{agg}}}} = \sqrt{\exp\left(H^2 + 2M\right)\left(\exp\left(H^2\right) - 1\right)} \tag{S8}$$

The macroscopic scattering cross-section is therefore

$$\frac{d\Sigma}{d\Omega}_{\mathrm{polydisperse}}(q) = \int \frac{d\Sigma}{d\Omega}(q) p(N_{\mathrm{agg}}) dN_{\mathrm{agg}} \tag{S9}$$

Instrumental resolution for SANS has been taken into account according to Ref. 4. The macroscopic scattering function is convoluted with a resolution function $R\left(q, \sigma_q\right)$, which depends on wavelength spread, finite collimation of the beam and detector resolution

$$\frac{d\Sigma}{d\Omega}_{\mathrm{smeared}}(q) = \int R(q, \sigma_q) \frac{d\Sigma}{d\Omega}_{\mathrm{polydisperse}}(q) dq \tag{S10}$$

Figure S2 and S1 show the SANS and SAXS profiles of $\mathrm{d_3{-}PA_{1190}PSS_{70}}$ micelles fitted with the model described in equation S2. The model is able to describe the data sufficiently well. Table S3 shows the fit parameters as well as χ^2 of this fit together with the fits presented in the main manuscript.

Figure S3 shows the SANS profiles of $\mathrm{d_3{-}PA_{360}PSS_{400}}$ micelles fitted with the model described in equation S2. The data for the contrasts shown in sub-figure D–F are not well described by the model. Since the model in equation S2 does not take into account interaction between the chains in the corona, contrast where the scattering signal is dominated by the

corona are poorly described.

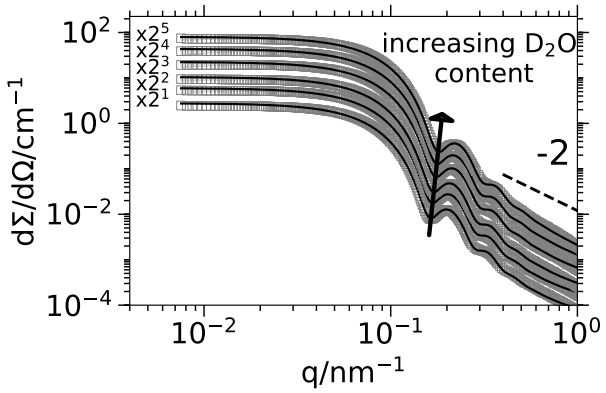

Figure S1: SAXS profiles of d_3−$PA_{1190}PSS_{70}$ micelles in 0.0%, 25.0%, 48.6% , 73.3%, 87.5% and 100.0% D_2O. The solid lines represent fits to equation S2.

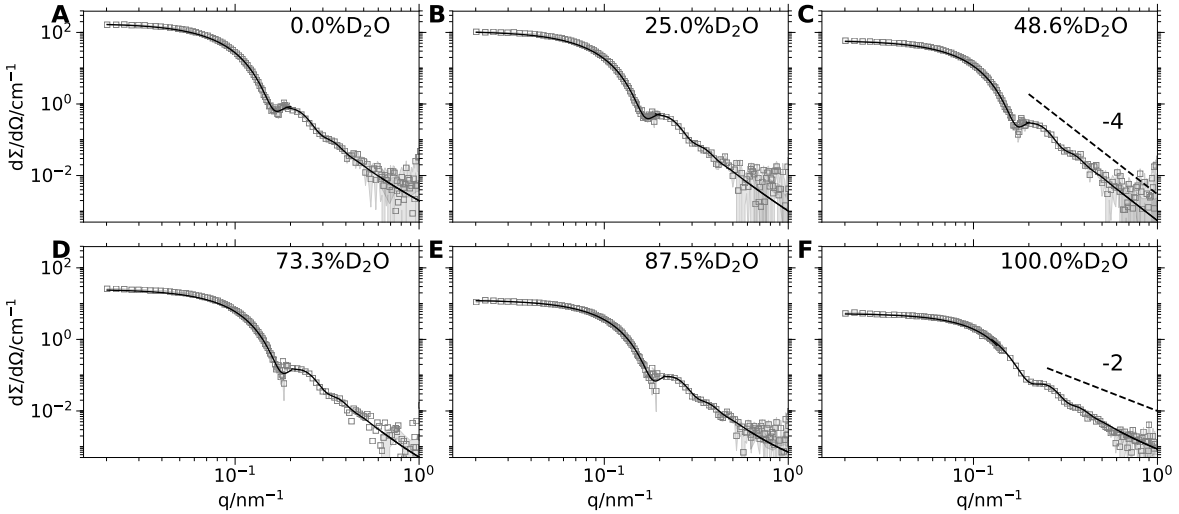

Figure S2: SANS profiles of d_3−$PA_{1190}PSS_{70}$ micelles in 0.0% D_2O (**A**), 25.0% D_2O (**B**), 48.6% D_2O (**C**), 73.3% D_2O (**D**), 87.5% D_2O (**E**) and 100.0% D_2O (**F**). The solid lines represent fits to equation S2.

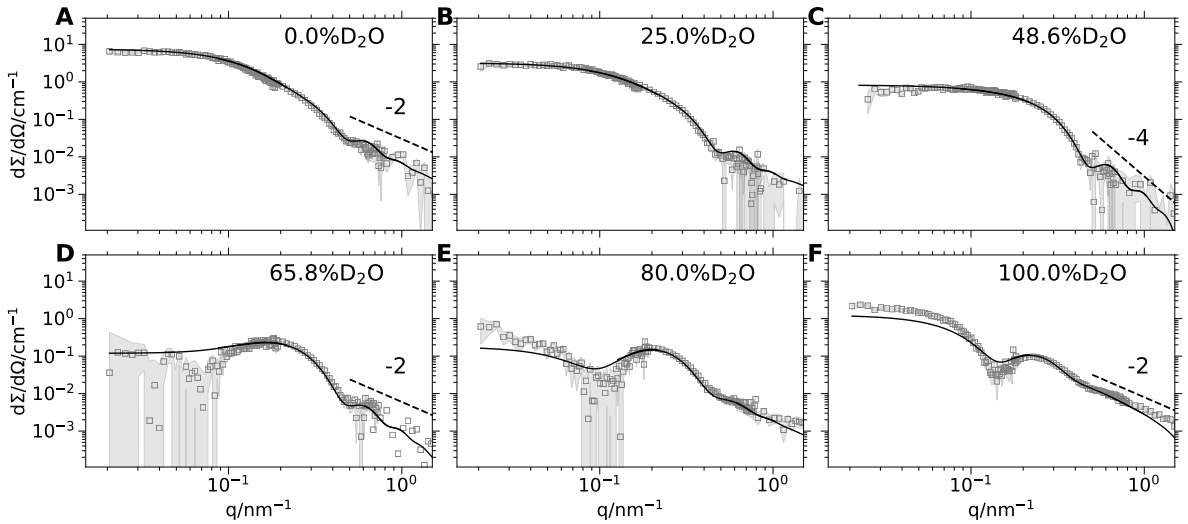

Figure S3: SANS profiles of $d_3-PA_{360}PSS_{400}$ micelles ($c_{poly} = 4\,g\,L^{-1}$, $c_{Ca^{2+}} = 50\,mmol\,L^{-1}$) in 0.0% D_2O (**A**), 25.0% D_2O (**B**), 48.6% D_2O (**C**), 65.8% D_2O (**D**), 80.0% D_2O (**E**) and 100.0% D_2O (**F**). The solid lines represent fits fit to equation S2.

3 Model with PSS core and d_3-PA corona

Figure S4 shows the SANS profiles of $d_3-PA_{360}PSS_{400}$ and the model fit (self-avoiding chains in the corona, c.f. equation 3 in the main manuscript) with PSS in the core and d_3-PA corona. This model can not describe the scattering data sufficiently well.

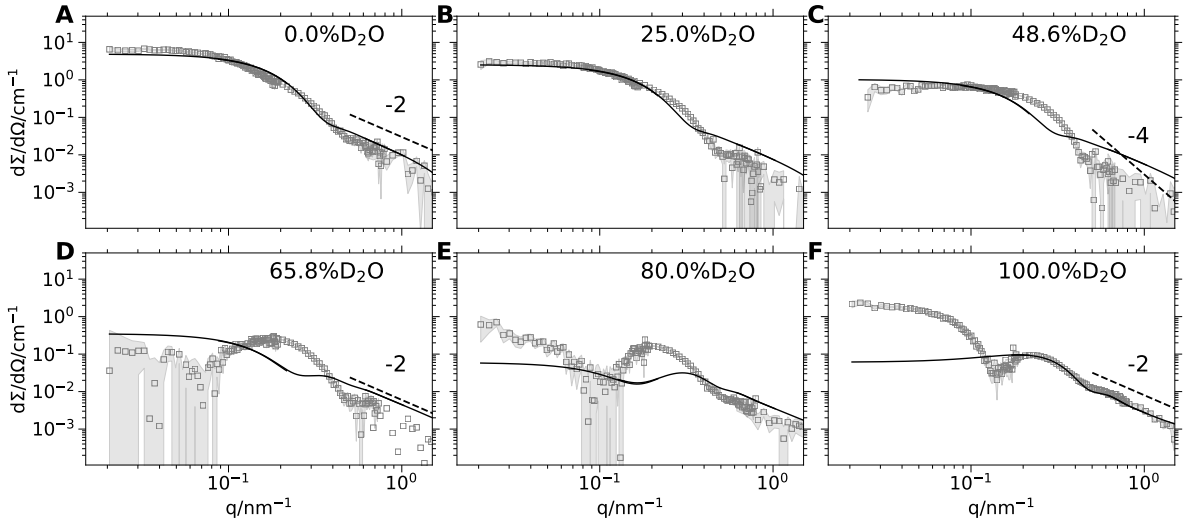

Figure S4: SANS profiles of d_3−$PA_{360}PSS_{400}$ ($c_{poly} = 4\,g\,L^{-1}$, $c_{Ca^{2+}} = 50\,mmol\,L^{-1}$) in 0.0% D_2O (**A**), 25.0% D_2O (**B**), 48.6% D_2O (**C**), 65.8% D_2O (**D**), 80.0% D_2O (**E**) and 100.0% D_2O (**F**). The solid lines represent fits to the form factor of a polydisperse block copolymer micelle with PSS in the core and d_3−PA in the corona.

4 Fitting procedure

For the form factor fits we used the SASET program,[5] which allows global fitting of several contrasts at the same time. During the data analysis of the SANS curves we took into account the instrumental resolution for each detector configuration and merged the data only for final representation. This approach allows us to increase the number of available data points since we do not truncate the data in the region of overlapping q. We performed a global fit to the SANS and SAXS data with a single set of shared fitting parameters. For the samples, where the aggregation number changes with D_2O content we attributed a common aggregation number to the corresponding SANS and SAXS curves but left the rest of the fitting parameters as global fitting parameters.

In order to constrain the fit we used the molar volumes of the individual blocks, known from the degree of polymerization and the molar volumes listed in Table S1. Moreover, we restricted the fit by giving the used polymer concentration. Together with the aggregation number N_{agg} (which is a fitting parameter) the number density N of micelles in L^{-1} is directly

obtained by

$$N = \frac{c}{M_{\text{polymer}} \text{N}_{\text{agg}}} N_A \tag{S11}$$

with c the polymer concentration in $\text{g}\,\text{L}^{-1}$, the molecular weight of the polymer M_{polymer} and the aggregation number N_{agg}.

5 Overview of the fit parameters from SANS and SAXS

Table S2 shows an overview of the obtained values of χ^2. Table S3 shows an overview of the obtained fitparameters for the SANS and SAXS profiles as well as the estimated errors. Note, that the error obtained from the least-squared fitting routine tends to underestimate the errors of the fit parameters. They also do not take into account systematic errors (e.g. from the difficult background subtraction for SAXS data at high q) and the correlation terms between the standard deviations of different fit parameters.[6]

Table S2: χ^2_{red} for the fits shown in the main manuscript (Figure 3, 4, 6, 7, 9 and 10) and Figure S2 and S1 in the supporting information.

Sample	Model	χ^2_{red}
$h_3-PA_{1190}PSS_{70}$	Self-avoiding chain	16.8
$d_3-PA_{1190}PSS_{70}$	Self-avoiding chain	55.0
$d_3-PA_{1190}PSS_{70}$	Gaussian chain	57.6
$d_3-PA_{360}PSS_{400}$	Self-avoiding chain	5.6

Table S3: Parameters for the micelles in the presence of $CaCl_2$ obtained for the fits shown in the main manuscript (Figure 3, 4, 5, 6, 7 and 8).

D_2O %		N_{agg}	$\sigma_{N_{agg}}/N_{agg}$	R_{core}/nm	$\sigma_{R_{core}}/R_{core}$	$R_{g,corona}$/nm	s/nm	ν	h	$V_{m,\ Ca^{2+}}$/cm^3 mol^{-1}	$\frac{d\Sigma}{d\Omega}_{inc}$/cm^{-1}
$h_3-PA_{1190}PSS_{70}$											
0.0	SANS	145.06 ± 0.20	$0.32 \pm 1.5 \cdot 10^{-4}$	23.98 ± 0.03	$0.105 \pm 4.8 \cdot 10^{-5}$	2.07 ± 0.02	$3.53 \pm 6.3 \cdot 10^{-3}$	$0.00 \pm 3.8 \cdot 10^{-3}$	10.22 ± 0.02	17.2 ± 0.03	$1.4 \cdot 10^{-2} \pm 2.4 \cdot 10^{-4}$
0.0	SAXS										—
25.0	SANS	144.90 ± 0.19		23.98 ± 0.03							$1.1 \cdot 10^{-3} \pm 1.8 \cdot 10^{-4}$
25.0	SAXS										—
48.6	SANS	134.19 ± 0.18		23.38 ± 0.03							$9.8 \cdot 10^{-4} \pm 1.3 \cdot 10^{-4}$
48.6	SAXS										—
54.0	SANS	132.65 ± 0.18		23.29 ± 0.03							$1.7 \cdot 10^{-3} \pm 5.8 \cdot 10^{-5}$
54.0	SAXS										—
73.3	SANS	126.35 ± 0.17		22.92 ± 0.03							$9.9 \cdot 10^{-4} \pm 4.9 \cdot 10^{-5}$
73.3	SAXS										—
100.0	SANS	116.80 ± 0.16		22.33 ± 0.03							$3.1 \cdot 10^{-13} \pm 3.5 \cdot 10^{-5}$
100.0	SAXS										—
$d_3-PA_{1190}PSS_{70}$											
0.0	SANS	168.40 ± 0.11	$0.31 \pm 1.5 \cdot 10^{-4}$	26.10 ± 0.02	$0.102 \pm 5.0 \cdot 10^{-5}$	2.12 ± 0.03	$4.05 \pm 8.9 \cdot 10^{-3}$	$0.00 \pm 7.4 \cdot 10^{-3}$	11.59 ± 0.01	13.9 ± 0.02	$2.7 \cdot 10^{-3} \pm 1.4 \cdot 10^{-4}$
0.0	SAXS										—
25.0	SANS	159.27 ± 0.10		25.63 ± 0.02							$1.3 \cdot 10^{-3} \pm 1.1 \cdot 10^{-4}$
25.0	SAXS										—
48.6	SANS	151.34 ± 0.11		25.20 ± 0.02							$2.1 \cdot 10^{-3} \pm 7.5 \cdot 10^{-5}$
48.6	SAXS										—
73.3	SANS	139.13 ± 0.09		24.51 ± 0.02							$1.5 \cdot 10^{-3} \pm 4.9 \cdot 10^{-5}$
73.3	SAXS										—
87.5	SANS	133.35 ± 0.09		24.17 ± 0.02							$1.7 \cdot 10^{-3} \pm 3.3 \cdot 10^{-5}$
87.5	SAXS										—
100.0	SANS	125.86 ± 0.08		23.71 ± 0.02							$2.8 \cdot 10^{-13} \pm 2.3 \cdot 10^{-5}$
100.0	SAXS										—
$d_3-PA_{360}PSS_{400}$											
0.0	SANS	19.6 ± 0.07	$0.21 \pm 9.9 \cdot 10^{-3}$	8.78 ± 0.03	$0.069 \pm 3.3 \cdot 10^{-3}$	9.55 ± 0.04	$8.86 \pm 9.5 \cdot 10^{-3}$	$1.19 \pm 2.3 \cdot 10^{-2}$	12.21 ± 0.03	19.6 ± 0.05	$2.0 \cdot 10^{-2} \pm 1.8 \cdot 10^{-4}$
0.0	SAXS										—
25.0	SANS										$4.4 \cdot 10^{-3} \pm 1.3 \cdot 10^{-4}$
25.0	SAXS										—
48.6	SANS										$4.4 \cdot 10^{-3} \pm 9.2 \cdot 10^{-5}$
48.6	SAXS										—
65.8	SANS										$3.0 \cdot 10^{-3} \pm 6.8 \cdot 10^{-5}$
65.8	SAXS										—
80.0	SANS										$1.5 \cdot 10^{-3} \pm 4.5 \cdot 10^{-5}$
80.0	SAXS										—
100.0	SANS										$8.6 \cdot 10^{-4} \pm 5.7 \cdot 10^{-5}$
100.0	SAXS										—

D_2O %		N_{agg}	$\sigma_{N_{agg}}/N_{agg}$	R_{core}/nm	$\sigma_{R_{core}}/R_{core}$	$R_{g,corona}$/nm	d		h	$V_{m,\ Ca^{2+}}$/cm^3 mol^{-1}	$\frac{d\Sigma}{d\Omega}_{inc}$/cm^{-1}
$d_3-PA_{1190}PSS_{70}$ with Gaussian chains in the corona											
0.0	SANS	163.81 ± 0.11	$0.31 \pm 1.5 \cdot 10^{-4}$	26.13 ± 0.02	$0.102 \pm 5.0 \cdot 10^{-5}$	3.11 ± 0.01	1		12.02 ± 0.01	13.8 ± 0.02	$2.7 \cdot 10^{-3} \pm 1.4 \cdot 10^{-4}$
0.0	SAXS										—
25.0	SANS	155.0 ± 0.09		25.65 ± 0.02							$1.3 \cdot 10^{-3} \pm 1.1 \cdot 10^{-4}$
25.0	SAXS										—
48.6	SANS	147.1 ± 0.10		25.22 ± 0.02							$2.1 \cdot 10^{-3} \pm 7.5 \cdot 10^{-5}$
48.6	SAXS										—
73.3	SANS	135.4 ± 0.08		24.54 ± 0.02							$1.5 \cdot 10^{-3} \pm 4.9 \cdot 10^{-5}$
73.3	SAXS										—
87.5	SANS	129.7 ± 0.09		24.19 ± 0.02							$1.7 \cdot 10^{-3} \pm 3.3 \cdot 10^{-5}$
87.5	SAXS										—
100.0	SANS	122.5 ± 0.08		23.73 ± 0.02							$2.8 \cdot 10^{-13} \pm 2.3 \cdot 10^{-5}$
100.0	SAXS										—

6 Fit with the form factor of a polydisperse sphere

A selection of three scattering curves, SANS curves recorded at 48.6 % D_2O and 100 % D_2O and one SAXS curve of $d_3{-}PA_{1190}PSS_{70}$ are fitted in addition by the simpler model of a polydisperse sphere[1] neglecting the corona. The results from these fits are illustrated in Figure S5. For the SANS curve recorded at the contrast at 48.6 % D_2O the data are well described as the corona is matched. However, the SANS curve at 100 % D_2O and the SAXS curve are poorly described at mid and high q. Hence, the SANS and SAXS data of $d_3{-}PA_{1190}PSS_{70}$ can not be adequately described by the model of a polydisperse sphere and an additional corona has to be taken into account.

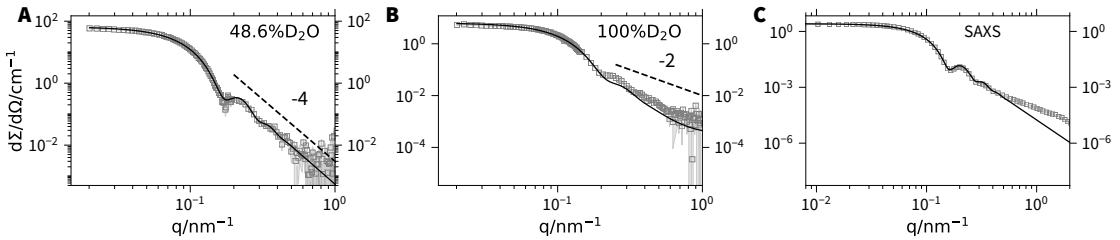

Figure S5: Fit of SANS and SAXS data of $d_3{-}PA_{1190}PSS_{70}$ micelles with the model of a polydisperse sphere.

References

(1) Rayleigh, L. Form factor of a homogenous sphere. *Proc. Roy. Soc. London* **1911**, *A84*, 25–38.

(2) Tondre, C.; Zana, R. Apparent molal volumes of polyelectrolytes in aqueous solutions. *J. Phys. Chem.* **1972**, *76*, 3451–3459, DOI: 10.1021/j100667a026.

(3) Pedersen, J. S.; Gerstenberg, M. C. Scattering Form Factor of Block Copolymer Micelles. *Macromolecules* **1996**, *29*, 1363–1365, DOI: 10.1021/ma9512115.

(4) Pedersen, J. S.; Posselt, D.; Mortensen, K. Analytical treatment of the resolution function for small-angle scattering. *J. Appl. Crystallogr.* **1990**, *23*, 321–333, DOI: 10.1107/S0021889890003946.

(5) Muthig, M.; Prévost, S.; Orglmeister, R.; Gradzielski, M. SASET: A program for series analysis of small-angle scattering data. *J. Appl. Crystallogr.* **2013**, *46*, 1187–1195, DOI: 10.1107/S0021889813016658.

(6) Press, W. H.; Teukolsky, S. A.; Vetterling, W. T.; Flannery, B. P. *Numerical recipes 3rd edition: The art of scientific computing*, 3rd ed.; Cambridge University Press, 2007.